Cattaneo-Christov Heat Flux Model of Eyring Powell Fluid Along with Convective Boundary Conditions

Bilal Ashraf, Muhammad*+

Department of Mathematics, COMSATS University Islamabad, Islamabad 44000, PAKISTAN

Sharma, Sapna; Aneja, Madhu

School of Mathematics, Thapar Institute of Engineering & Technology, Patiala-147004, INDIA

ABSTRACT: *Heat and mass transfer effects in three-dimensional mixed convection flow of Eyring Powell fluid over an exponentially stretching surface with convective boundary conditions are inspected. Cattaneo-Christov Heat Flux model is a modified version of the classical Fourier's law that takes into account the interesting aspect of thermal relaxation time. First-order chemical reaction effects are also taken into account. Similarity transformations are invoked to reduce the leading boundary layer partial differential equations into the ordinary differential equations. The nonlinear, coupled ordinary differential with boundary conditions has been analyzed numerically by using the Finite Element Method.*

INTRODUCTION

Glass blowing, continuous casting of metals, and spinning of fibers involve the flow due to a stretching surface in an ambient fluid. The quality of the final sheeting material, as well as the cost of production is affected by the speed of collection and the heat transfer rate. Also, in several engineering processes, materials manufactured by extrusion processes and heat-treated materials traveling between a feed roll and a wind-up roll-on convey belts possess the characteristic of a moving continuous surface. After the initial contribution of *Crane* [1], various researchers extended the flow over a stretching surface in directions of Newtonian and non-Newtonian fluid models under different geometries. Mechanics of non-Newtonian fluid flows present a special challenge to engineers, physicists, and mathematicians. Because of the complexity of these fluids, there is not a single constitutive equation that exhibits all properties of such non-Newtonian fluids. In the process, a number of non-Newtonian fluid models have been proposed. In the literature, the vast majority of non-Newtonian fluid are concerned of the types, e.g., the power-law [2], viscoelastic fluid [3], grade two or three [4], Maxwell fluid [5]. Flow problems involve the exponential dependence of the similarity variables as the stretching velocity and temperature distribution are presented by exponentially stretching the surface. Mostly the researchers

presented the solutions for two-dimensional exponentially stretching flows. Thermal boundary layer over an exponentially stretching continuous surface with magnetic field effect was investigated numerically by *Al-Odat et al.* [6]. Analytical solutions of nanofluid flow over an exponential stretching surface were presented by *Nadeem* and *Lee* [7]. Heat transfer analysis over an exponentially shrinking surface by applying shooting method was investigated by *Bhattacharyya* [8]. Heat transfer over a permeable stretching surface for a Casson fluid was studied by *Mukhopadhyay et al.* [9]. After that, Three-dimensional viscous flow in presence of heat transfer over an exponentially stretching surface is studied by *Liu et al.* [10]. Recently *Ashraf et al.* [11] extended the flow of *Liu et al.* [10] by considering the viscoelastic fluid.

Many investigators stressed on the magnetohydrodynamic flow of an electrically conducting fluid because of numerous applications in metallurgical industry such as in drawing, annealing, in the purification of molten metals from non-metallic inclusions, electromagnetic pumps, MHD generators etc. Several studies have been presented by the authors in presence of transverse magnetic field over a stretching surface. Magnetohydrodynamic boundary layer flow with variable viscosity over a stretching surface was presented by *Mukhopadhyay et al.* [12]. *Motsa et al.* [13] obtained the solutions for upper convected Maxwell fluid over porous stretching sheet in presence of magnetic field by using successive Taylor series linearization method. *Rashidi* and *Erfani* [14] studied the stagnation-point flow in porous media with magnetic field.

Heat conduction is a widespread nature phenomenon occurring in many fields [16-21]. The classical heat conduction equation is based on the Fourier law. The classical Fourier law has been highly successful in a very wide range of engineering applications. However, one unphysical property is that it issues an infinite velocity of propagation, i.e., any initial disturbance is felt instantly throughout the whole of the medium. In order to overcome this problem, *Cattaneo* [22] modified the Fourier law by taking the finite velocity of propagation into account. This extension turns the diffusion equation from a parabolic equation to a hyperbolic one. In recent years, many researchers devoted themselves to the study of heat conduction with Cattaneo model. *Christov* and *Jordan* [23] pointed out that the usual form of Maxwell-Cattaneo leads to a paradoxical result if the body is in motion,

the governing equation cannot be reduced to a single transport equation in the multidimensional case. *Qi* and *Guo* [24] studied the initial-boundary value problem of general-ized Cattaneo equation, the exact solution was obtained in series forms in terms of the H-function by utilizing the Laplace transform. *Compte* and *Metzler* [25] generalized the Cattaneo equation to study the anomalous transport, three possible generalizations were pro-posed which can be used to describe continuous time random walks, non-local transport theory, and delayed flux-force relation. *Straughan* [26] investigated convection effects in the horizontal layer of incompressible fluid over a flat plate utilizing Cattaneo--Christov heat flux. *Tibullo* and *Zampoli* [27] proved existence and uniqueness of solutions for equations governing heat transfer in incompressible fluids through Cattaneo--Christov theory. *Haddad* [28] examined thermal instability in Brinkman porous media considering non-Fourier heat flux.

Thus purpose of present research is to study the three dimensional flow of Eyring Powell fluid with convective boundary conditions by using Finite Element Method [29-32]. The novelty. Many authors investigated three dimensional flow of Erying Powell fluid over a stretching sheet with different boundary conditions [33, 34]. The novelty of the problem is to investigate Catteneo-Christov heat flux model for three dimensional flow of Erying Powell fluid. Here the temperature and thermal boundary layer thickness are lower for Cattaneo-Christov heat flux model in comparison to classical Fourier's law of heat conduction. Impacts of embedding parameters on the flow and temperature fields are examined graphically. Numerical values of skin-friction coefficient, transversal skin-friction coefficient and local Nusselt number for sundry variables are obtained and discussed.

THEORETICAL SECTION
Mathematical modeling

We consider the three-dimensional boundary layer flow of Eyring Powell nanofluid by an exponentially stretching surface. The surface coincides with the plane $z = 0$ and the flow is confined in the region $z > 0$. Heat and mass transfer effects are taken into account. Effects of Brownian motion and thermophoresis are considered. The Cauchy stress tensor T for an Eyring Powell Fluid can be written as [33]:

$$T = pI + \tau_{ij} \tag{1}$$

$$\rho\, a_i = -\nabla p + \nabla . \tau_{ij} \tag{2}$$

where extra stress tensor τ_{ij} is given by

$$\tau_{ij} = \mu \frac{\partial u_i}{\partial x_j} + \frac{1}{\beta} \sinh^{-1}\left(\frac{1}{c}\frac{\partial u_i}{\partial x_j} \right) \tag{3}$$

in which β and c are the Eyring Powell fluid characterstics, p is the pressure and I is the identity tensor. Taking

$$\sinh^{-1}\left(\frac{1}{c}\frac{\partial u_i}{\partial x_j} \right) \approx \frac{1}{c}\frac{\partial u_i}{\partial x_j} - \frac{1}{6}\left(\frac{\partial u_i}{\partial x_j} \right)^3 \quad ; \quad \left| \frac{1}{c}\frac{\partial u_i}{\partial x_j} \right| < 1 \tag{4}$$

The governing equations for the three-dimensional flow can be put into the form:

$$\frac{\partial u}{\partial x} + \frac{\partial v}{\partial y} + \frac{\partial w}{\partial z} = 0 \tag{5}$$

$$u\frac{\partial u}{\partial x} + v\frac{\partial u}{\partial y} + w\frac{\partial u}{\partial z} = \left(\vartheta + \frac{1}{\beta c \rho} \right)\frac{\partial^2 u}{\partial z^2} - \tag{6}$$

$$\frac{1}{2\beta c^3 \rho}\left(\frac{\partial u}{\partial z} \right)^2 \frac{\partial^2 u}{\partial z^2} - \frac{\sigma^* B_0^2}{\rho} u + g\beta_e \left(T - T_\infty \right) + g\beta_c \left(C - C_\infty \right)$$

$$u\frac{\partial v}{\partial x} + v\frac{\partial v}{\partial y} + w\frac{\partial v}{\partial z} = \left(\vartheta + \frac{1}{\beta c \rho} \right)\frac{\partial^2 v}{\partial z^2} - \tag{7}$$

$$\frac{1}{2\beta c^3 \rho}\left(\frac{\partial v}{\partial z} \right)^2 \frac{\partial^2 v}{\partial z^2} - \frac{\sigma^* B_0^2}{\rho} v$$

$$\left(\rho c_p \right)\left(u\frac{\partial T}{\partial x} + v\frac{\partial v}{\partial y}T + w\frac{\partial T}{\partial z} \right) = -\nabla . q \tag{8}$$

$$u\frac{\partial c}{\partial x} + v\frac{\partial c}{\partial y} + w\frac{\partial c}{\partial z} = D_B \frac{\partial^2 C}{\partial z^2} + \frac{D_T}{T_\infty}\frac{\partial^2 T}{\partial z^2} - \tag{9}$$

$$k_1 \left(C - C_\infty \right)$$

The modified form of Fourier law of heat conduction i.e. Catteneo – Christov heat flux model is utilized for the case of incompressible flows in which heat flux q is given by [35]

$$q + \lambda_1 \left[\frac{\partial y}{\partial x} + V.\nabla q - q.\nabla v \right] = -K\nabla T \tag{10}$$

We eliminate q from equations (8) and (10) to obtain the following:

$$u\frac{\partial T}{\partial x} + v\frac{\partial T}{\partial y} + w\frac{\partial T}{\partial z} = \frac{K}{\rho c_p}\frac{\partial^2 T}{\partial x^2} - \tag{10}$$

$$\lambda_1 \left(u^2\frac{\partial^2 T}{\partial x^2} + v^2\frac{\partial^2 T}{\partial y^2} + w^2\frac{\partial^2 T}{\partial z^2} + 2uv\frac{\partial^2 T}{\partial x \partial y} + 2vw\frac{\partial^2 T}{\partial y \partial z} + \right.$$

$$2uw\frac{\partial^2 T}{\partial z \partial x} + \left(u\frac{\partial u}{\partial x} + v\frac{\partial u}{\partial y} + w\frac{\partial u}{\partial z} \right)\frac{\partial T}{\partial x} +$$

$$\left. \left(u\frac{\partial u}{\partial x} + v\frac{\partial u}{\partial y} + w\frac{\partial u}{\partial z} \right)\frac{\partial T}{\partial x} + \left(u\frac{\partial u}{\partial x} + v\frac{\partial u}{\partial y} + w\frac{\partial u}{\partial z} \right)\frac{\partial T}{\partial z} \right)$$

The corresponding boundary conditions are [15]:

$$u = U_w \quad , \quad v = V_w \quad , \quad w = 0$$

$$-K\frac{\partial T}{\partial z} = h\left(T_f - T \right), \; -D\frac{\partial T}{\partial z} = h^*\left(C_f - C \right) \quad \text{at} \tag{12}$$

$$z = 0$$

$$u \to 0, \; v \to 0, \; T \to T_\infty, \; C \to C_\infty \quad \text{as}$$

$$z \to z_\infty$$

The velocities, temperature and concentration at the wall are [33]:

$$U_w = U_0 e^{\frac{x+y}{L}} \quad , \quad V_w = V_0 e^{\frac{x+y}{L}} \quad , \tag{13}$$

$$T_w = T_\infty + T_0 e^{\frac{A(x+y)}{2L}} \quad , \quad C_w = C_\infty + C_0 e^{\frac{B(x+y)}{2L}}$$

The following transformations are used to convert the governing equations of the flow problem into non-dimensionalized form [33]:

$$u = U_0 e^{\frac{x+y}{L}} f'(\eta) \quad , \quad v = U_0 e^{\frac{x+y}{L}} g'(\eta) \tag{14}$$

$$w = -\left(\frac{\vartheta U_0}{2L} \right)^{1/2} e^{\frac{x+y}{2L}}\left(f + \eta f' + g + \eta g' \right)$$

$$T = T_\infty + T_0 e^{\frac{A(x+y)}{2L}} \theta(\eta) \quad , \quad \eta = \left(\frac{U_0}{2\vartheta L} \right)^{1/2} e^{\frac{x+y}{2L}} z$$

$$C_w = C_\infty + C_0 e^{\frac{B(x+y)}{2L}} \varphi(\eta)$$

The Eq. (5) is automatically satisfied with above mentioned transformations and Eqs (6-11) in non-dimensionalized form are:

$$\left(1 + \in \right)f''' + \left(f + g \right)f'' - 2\left(f' + g' \right)f' - \tag{15}$$

$$\in \delta \left(f'' \right)^2 f''' - Mf' + \lambda_e \theta + \lambda_c \varphi = 0$$

$$(1 + \epsilon) g''' + (f + g) g'' - 2 (f' + g') g' - \quad (16)$$

$$\epsilon \delta (g'')^2 g''' - M g' = 0$$

$$\frac{1}{Pr} \theta'' + \frac{\gamma}{2} \Big(A \theta (f + g)(f'' + g'') - \quad (17)$$

$$A \theta (2 + A)(f' + g')^2 + (1 + 2A)(f' + g')(f + g) \theta' -$$

$$(f + g)^2 \theta'' \Big) - A \theta (f' + g') + \theta'(f + g) = 0$$

$$\varphi'' + Sc (f + g) \varphi' - ScB (f' + g') \varphi + \frac{Nt}{Nb} \theta'' - Sck\varphi = 0 \quad (18)$$

The boundary conditions (12) in non-dimensionalized form are:

$$f = 0, \; g = 0, \; f' = 1, \; g' = \epsilon, \; \theta' = -\gamma_1 (1 - \theta(0)) \quad (19)$$

$$\varphi' = -\gamma_2 (1 - \varphi(0)) \quad at \quad \eta = 0 \quad and$$

$$f' \to 0, \; g' \to 0, \; \theta \to 0, \; \varphi \to 0 \quad as \quad \eta \to \infty$$

The various non-dimensional number mentioned in the above equations are mentioned in nomenclature and are defined as:

$$\epsilon = \frac{1}{\mu \beta_c}, \quad \delta = \frac{U_0^3 e^{\frac{3(x+y)}{L}}}{2\vartheta c^2 l}, \quad Pr = \frac{\vartheta}{\alpha}, \quad (20)$$

$$Nb = \frac{\rho^* c_p^* D_B (C_w - C_\infty)}{\rho c \vartheta}, \quad k = \frac{k_1}{U_0}, \quad M = \frac{\sigma^* \rho}{B_0^2},$$

$$Nt = \frac{\rho^* c_p^* D_B (T_w - T_\infty)}{\rho c T_\infty \vartheta}, \quad Sc = \frac{\vartheta}{D_B}, \quad \omega = \frac{V_0}{U_0},$$

$$\gamma_1 = \frac{h}{k} \sqrt{\frac{\vartheta}{a'}}, \quad \gamma_2 = \frac{h^*}{D} \sqrt{\frac{\vartheta}{a'}}, \quad \gamma = \frac{\lambda_1 U_0 e^{\frac{x+y}{L}}}{L}$$

The quantity of physical interest are local Nusselt number and local Sherwood number which are defined as

$$\frac{Nu}{Re_x^{1/2}} = -\frac{x}{2L} \theta'(0), \quad \frac{Sh}{Re_x^{1/2}} = -\frac{x}{2L} \varphi'(0) \quad (21)$$

Where $Re_x = \frac{U_0 L}{\vartheta} e^{\frac{x+y}{L}}$ is the local Reynolds number.

Solution Approach

The system of nonlinear ordinary differential Eqs (15 - 18) subjected to boundary conditions (19) has been solved

numerically by finite element method. Momentum Eqs (15, 16) is third order coupled equations. So, these equations are solved in the coupled form. In order to convert third order equation into second order, we assume:

$$f' = h \quad (22)$$

$$g' = l \quad (23)$$

$$(1 + \epsilon) h'' + (f + g) h' - 2 (f' + g') f' - \epsilon \delta (h')^2 h'' - \quad (24)$$

$$M f' + \lambda_e \theta + \lambda_c \varphi = 0$$

$$(1 + \epsilon) l'' + (f + g) l' - 2 (f' + g') g' - \quad (25)$$

$$\epsilon \delta (l')^2 l'' - M g' = 0$$

$$\frac{1}{Pr} \theta'' + \frac{\gamma}{2} \Big(A \theta (f + q)(h' + l') - A \theta (2 + A)(f' + g')^2 + \quad (26)$$

$$(1 + 2A)(f' + g')(f + g) \theta' - (f + g)^2 \theta'' \Big) -$$

$$A \theta (f' + g') + \theta'(f + g) = 0$$

$$\varphi'' + Sc (f + g) \varphi' - ScB (f' + g') \varphi + \frac{Nt}{Nb} \theta'' - Sck\varphi = 0 \quad (27)$$

$$f = 0, \; g = 0, \; h = 1, \; l = \alpha, \; \theta' = -\gamma_1 (1 - \theta(0)) \quad (28)$$

$$\varphi' = -\gamma_2 (1 - \varphi(0)) \quad at \quad \eta = 0 \quad and \quad f' \to 0,$$

$$g' \to 0, \; \theta \to 0, \; \varphi \to 0 \quad as \quad \eta \to \infty$$

A grid independence test is performed by taking uniform grid of different sizes such as 80, 100, 120, 140 nodes. The results are not much affected by varying grid size. So, results are obtained by taking 120 nodes of uniform size. Also results has been validated with previous obtained results by *Bilal et al.* [33] by considering special case in which thermal relaxation time $\gamma = 0$ and is presented in Fig. 1.

RESULTS AND DISCUSSION

The nonlinear, coupled ordinary differential Eqs. (15 - 18) with boundary conditions (19) has been analyzed numerically using FEM. The influence of important parameters such as Eyring Powell fluid parameters ϵ, δ, relaxation time for heat flux γ, heat and mass transfer Biot number γ_1 and γ_2, Prandtl number Pr, Brownian motion parameter Nb, Thermophoresis parameter Nt are analyzed on velocity profile, temperature profile, concentration
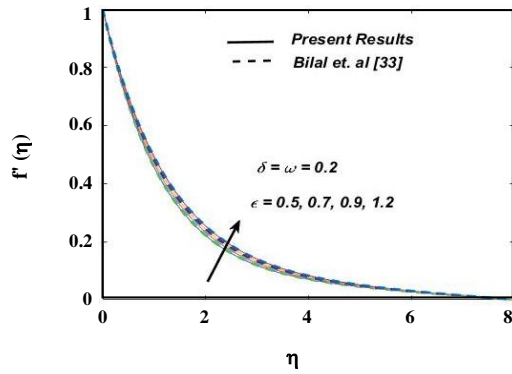
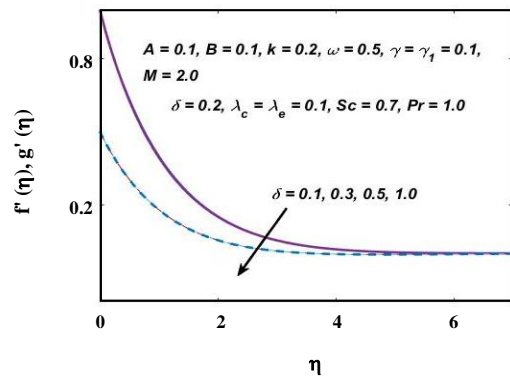*Fig 1: Validation of results with previous studies.*
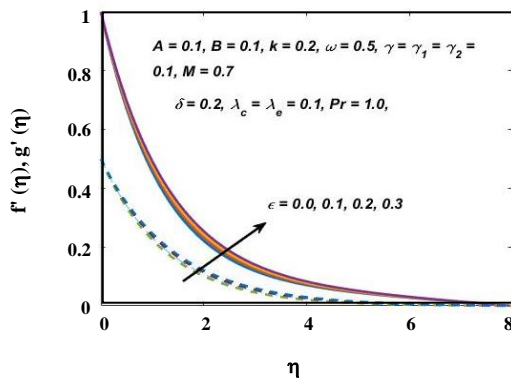

Fig 3: Effect of δ on velocity profile.
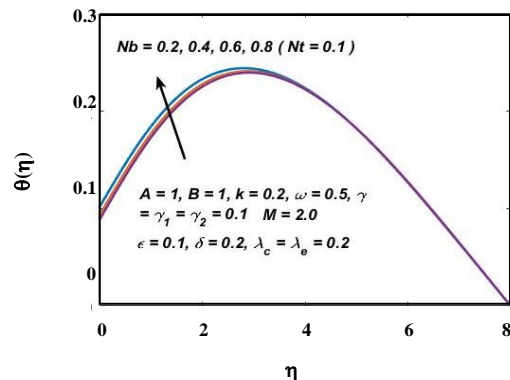

Fig 2: Effect of ϵ on velocity profile.

Fig 4: Effect of Nb on temperature profile.

profile graphically. Fig. 2 describes the velocity profile for different values of ϵ. Since $\epsilon = \frac{1}{\rho\beta_c}$ so by increasing ϵ viscosity of fluid decreases, which causes increase in velocity. Fig. 3 reflects the effect of δ on velocity profile. It is depicted that velocity decreases with increase in δ. This is due to the fact that viscosity of fluid increases with increase in δ which causes decrease in velocity profile.

Figs. 4-8 show the variation of temperature field $\theta(\eta)$ for different values of Brownian motion parameter Nb, thermophoresis paramter Nt, relaxation time for heat flux γ, heat transfer Biot number γ_1, Prandtl number Pr. Fig. 4 show the variation of temperature profile and boundary layer thickness for increasing values of Nb. Random motion of fluid increases by increasing the Brownian motion parameter Nb. Thus fluid particles frequently strike with each other which produces more heat so it raises temperature.

Fig. 5 shows characteristics of thermophoresis parameter Nt on temperature profile. Thermophoresis is a mechanism in which small particles are pulled away from hot surface to cold surface. Due to this transportation

temperature of the fluid rises. This is also happened because additional heat is generated due to the interaction of nano-particles with the base fluid due to Brownian motion and thermophoresis effects. This results in depletion of thermal boundary layer thickness and hence the temperature overshoots are observed in the vicinity of the stretching sheet for increasing value of Nb and Nt. Fig. 6 depicts that temperature reduces when thermal relaxation time for heat flux increases γ. Physically when γ increases the material particles need extra time to transfer heat to its adjacent particles, thus temperature reduces. Fig. 7 shows that a pronounced increase in the temperature and corresponding boundary layer thickness when there is an increase in heat transfer Biot number γ_1. Fig. 8 shows the impact of Prandtl number Pr on temperature profile. Since $Pr = \frac{\vartheta}{\alpha}$, thus by increasing Prandtl number Pr thermal conductivity of fluid decreases which reduces temperature profile. Additionally, an increase in Prandtl number reduces thermal boundary layer thickness. So heat rapidly transfers which causes a drop in fluid temperature.
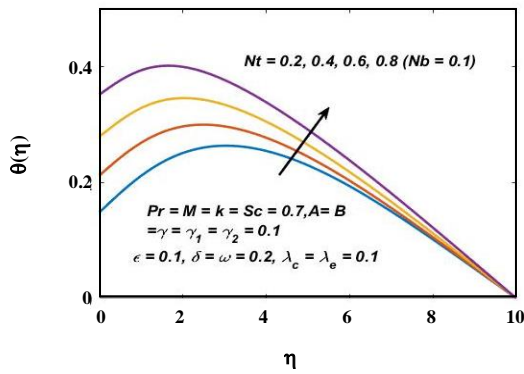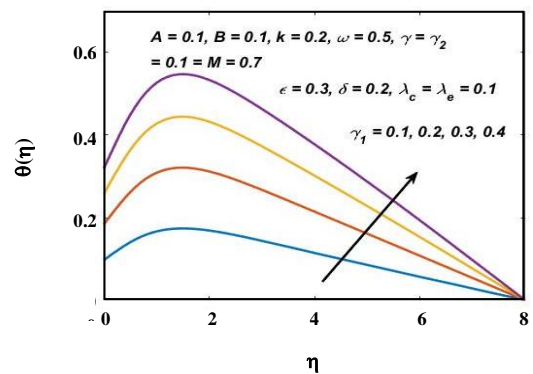
Fig. 5: Effect of Nt on temperature profile.

Fig. 7: Effect of γ_1 on temperature profile.
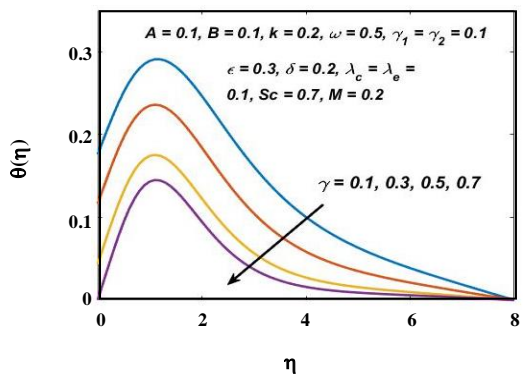

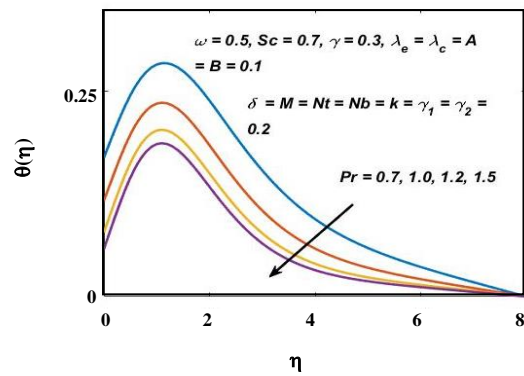**Fig 6: Effect of γ on temperature profile.**

Fig. 8: Effect of Pr on temperature profile.

Figs. 9-11 shows the variation in concentration profile for different values of Schmidt number Sc, chemical reaction parameter k and mass transfer Biot number γ_2. Fig 9 reveals that when Schmidt number increases, it causes decrease in concentration, higher value of Schmidt number lowers the mass diffusivity. Due to this thickness of concentration boundary layer declines. Fig. 10 reveals the influence of chemical reaction parameter k on concentration profile. It shows that concentration decreases with the increase in parameter k. This is because the higher the reaction rate, the thicker the concentration boundary layer. It is observed in Fig. 11 that concentration profile rises when mass transfer Biot number γ_2 increases.

Impacts of parameters ϵ and δ, Brownian motion parameter Nb, Thermophoresis parameter Nt on Nusselt number $-\theta'(0)$ are depicted in Figs. 12, 13. Fig. 12 is drawn to examine the variations of ϵ and δ on Nusselt number $-\theta'(0)$. Nusselt number increases with an increase in ϵ while Nusselt reduces with an enhancement in δ. It is

shown in Fig. 13 that with variations in Nb and Nt Nusselt number increases.

Fig. 14 shows the variation of parameters ϵ and δ on Sherwood number $-\varphi'(0)$. It is analyzed that Sherwood number rises with an increase in ϵ while it reduces with δ.

CONCLUSIONS

In the present study Catteneo-Christov heat flux model is considered for three dimensional flow of Erying Powell fluid. The following observations in the existing study is worth mentioning:

1- Velocity profile in in x and y direction increases with increase in ϵ while reverse pattern is observed for increasing value of δ.

2- Temperature rises with enhancement in Nb, Nt and γ_1 while it decreases with increment in thermal relaxation time γ.

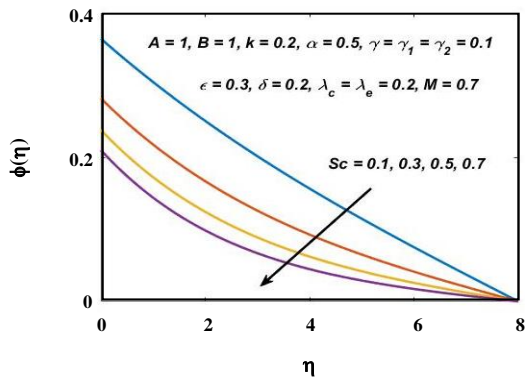3- Concentration profile decreases with increase in Sc (Schmidt number) and k (chemical reaction parameter).
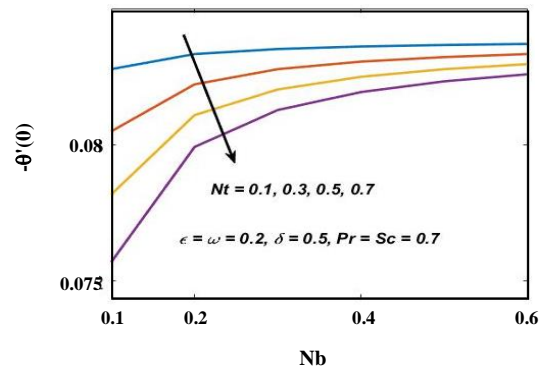
Fig. 9: Effect of Sc on concentration profile.

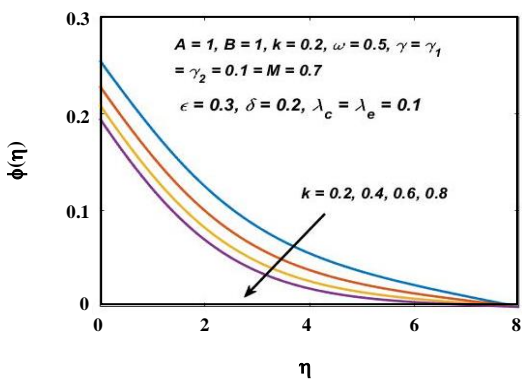*Fig. 12: Effect of ϵ and δ on Nusselt number.*

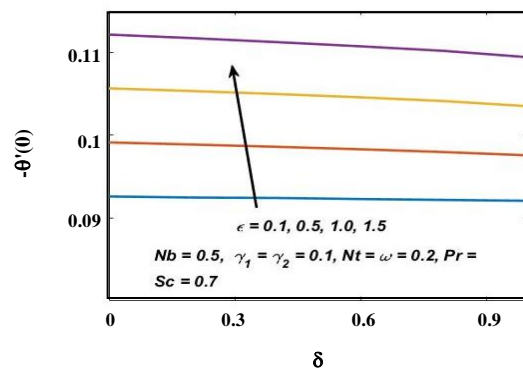*Fig 10: Effect of k on concentration profile.*

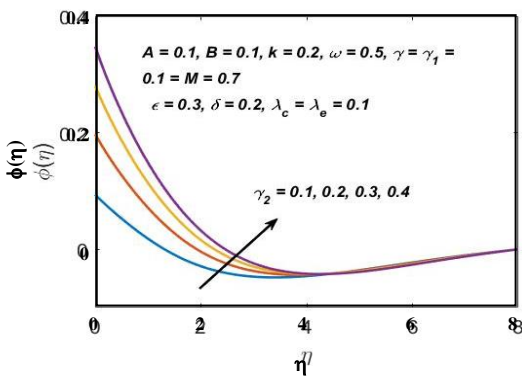*Fig. 13: Effect of Nb and Nt on Nusselt number.*

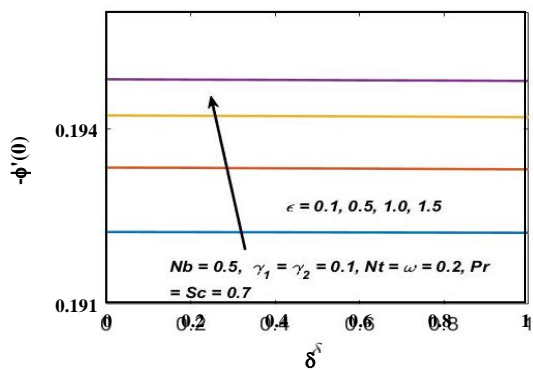*Fig. 11: Effect of γ_2 on concentration profile.*

Fig. 14: Effect of ϵ and δ on Sherwood number.

On the other it enhances with mass transfer Biot number γ_2.

4- Rate of heat transfer i.e., Nusselt number decreases with Nt and it increases with ϵ.

5- Rate of mass transfer i.e., Sherwood number remains almost constant for different values of δ while it rises with ϵ.

Nomenclature

A	Temperature exponent
B	Concentration exponent
c	Erying Powell fluid characteristics
c_p	Specific heat of the fluid
C_f	Ambient fluid concentration

h	Heat transfer coefficient
h^*	Concentration transfer coefficient
M	Hartman number
T_f	Ambient fluid temperature
Sc	Schmidt number
g	Gravitational acceleration constant
k	Chemical reaction parameter
K	Thermal conductivity of the fluid
Nu	Local Nusselt number
Nb	Brownian motion parameter
Nt	Thermophoresis parameter
p	Pressure
Pr	Prandtl number
q	Heat flux
Re_x	Local Reynolds number
Sh	Local Sherwood number
T	Temperature
u, v, w	Velocity components in x, y and z-direction

Greek Symbols

α	Thermal diffusivity
β	Erying Powell fluid characteristics
β_c	Concentration expansion coefficient
β_e	Thermal expansion coefficient
γ	Non-dimensional relaxation time
γ_1	Heat transfer Biot number
γ_2	Mass transfer Biot number
δ	Erying Powell fluid parameter
ϵ	Erying Powell fluid parameter
ω	Ratio of stretching velocities
λ_1	Thermal relaxation time
λ_e	Thermal buoyancy parameter
λ_c	Solutal buoyancy parameter
ϑ	Kinematic viscosity
ρ	Fluid's density
σ	Electrical conductivity
$\theta(\eta)$	Dimensionless temperature
$\varphi(\eta)$	Dimensionless concentration

Subscripts

$(\,)_w$	Wall conditions
$(\,)_\infty$	Free stream conditions

REFERENCES

[1] Crane L. J., Flow Past a Stretching Plate, *J. App. Math Phys. (ZAMP),* **21**: 645-647 (1970).

[2] Andersson H.I., Bech K.H., Dandapat B.S., Magnetohydrodynamic flow of a power-law fluid over a stretching sheet, *Int. J. Non-Lin. Mech.*, **27(6)**: 929-936 (1992).

[3] Hayat T., Ashraf M.B., Alsulami H.H., Alhuthali M.S., Three-Dimensional Mixed Convection Flow of Viscoelastic Fluid with Thermal Radiation and Convective Conditions, *Plos. One.*, **9(3)**: e90038 (2014).

[4] Aksoy Y., Pakdemirli M., Khalique C.M., Boundary-Layer Equations and Stretching Sheet Solutions for the Modified Second Grade Fluid, *Int. J. Eng. Sci.*, **45(10)**: 829-41 (2007).

[5] Bilal Ashraf M, Hayat T, Alhuthali M.S., Three-Dimensional Flow of Maxwell Fluid with Soret and Dufour Effects, *J. Aerospace Eng.*, **29(3)**: 04015065 (2015).

[6] Al-Odat M.Q., Damesh R.A., Al-Azab T.A., Thermal Boundary Layer on an Exponentially Stretching Continuous Surface in the Presence of Magnetic Field, *Int. J. App. Mech. Eng.*, **11**: 289-299 (2006).

[7] Nadeem S., Lee C., Boundary Layer Flow of Nanofluid over an Exponentially Stretching Surface, *Nanoscale Res. Lett.*, **7**: 94 (2012).

[8] Bhattacharyya K., Boundary Layer Flow and Heat Transfer over an Exponentially Shrinking Sheet, *Chinese Phys. Lett.*, **28**: 074701 (2011).

[9] Mukhopadhyay S., Vajravelu K., Gorder R.A.V., Casson Fluid Flow and Heat Transfer at an Exponentially Stretching Permeable Surface, *J. App. Mech.*, **80**: 054502 (2013).

[10] Liu I.C., Wang H.H., Peng Y.F., Flow and Heat Transfer for Three Dimensional Flow over an Exponentially Stretching Surface, *Chem. Eng. Comm.*, **200**: 253-268 (2013).

[11] Bilal Ashraf M., Hayat T., Shehzad S.A., Malaikah H., Three Dimensional Flow of a Viscoelastic Fluid on an Exponentially Stretching Surface, *J. App. Mech. Tech. Phys.*, **57**: 446-456 (2016).

[12] Mukhopadhyay S., Layek G.C., Samad S.K.A, Study of MHD Boundary Layer Flow over a Heated Stretching Sheet with Variable Viscosity, *Int. J. Heat Mass Trans.,* **48**: 4460-4466 (2005).

Research Article

[13] Motsa S.S., Hayat T., Aldossary O.M., MHD Flow of Upper- Convected Maxwell Fluid over Porous Stretching Sheet Using Successive Taylor Series Linearization Method, *Appl. Math Mech.*, **33**: 975-990 (2012).

[14] Rashidi M.M., Erfani E., A New Analytical Study of MHD Stagnation-Point Flow in Porous Media with Heat Transfer, *Comput. Fluids*, **40**: 172-178 (2011).

[16] Howell J.R., Menguc M.P., Siegel R., "Thermal Radiation Heat Transfer", CRC Press, (2015).

[17] Sheikholeslami M, Haq R.U, Shafee A., Li Z., Elaraki Y.G., Tlili I, Heat Transfer Simulation of Heat Storage Unit with Nanoparticles and Fins Through a Heat Exchanger, *Int. J. Heat Mass Trans.,* **135**:470-8 (2019).

[18] Sheikholeslami M, Haq R.U., Shafee A., Li Z, Heat Transfer Behavior of Nanoparticle Enhanced PCM Solidification Through an Enclosure with V-Shaped Fins, *Int. J. Heat Mass Trans*, **130**:1322-42 (2019).

[19] Sheikholeslami M., Rezaeianjouybari B., Darzi M., Shafee A., Li Z., Nguyen T.K., Application of Nano-Refrigerant for Boiling Heat Transfer Enhancement Employing an Experimental Study, *Int. J. Heat Mass Trans.*, **141**: 974-80 (2019).

[20] Sheikholeslami M., Jafaryar M., Hedayat M., Shafee A., Li Z., Nguyen T.K., Bakouri M, Heat Transfer and Turbulent Simulation of Nanomaterial Due to Compound Turbulator Including Irreversibility Analysis, *Int. J. Heat Mass Trans.*, **137**: 1290-300 (2019).

[21] Sheikholeslami M., Jafaryar M., Shafee A, Li Z., Haq R.U., Heat Transfer of Nanoparticles Employing Innovative Turbulator Considering Entropy Generation, *Int. J. Heat Mass Trans.*, **136**: 1233-40 (2019).

[22] Cattaneo C., Sulla Conduzione Del Calore, *Atti Semin. Mat. Fis. Univ. Modena Reggio Emilia*, **3**: 83-101 (1948).

[23] Christov C.I., Jordan P.M., Heat Conduction Paradox Involving Second-Sound Propagation in Moving Media, *Phys. Rev. Lett.*, **94**: 154301 (2005).

[24] Qi H., Guo X., Transient Fractional Heat Conduction with Generalized Cattaneo Model, *Int. J. Heat Mass Trans.*, **76**: 535-539 (2014).

[25] Compte A, Metzler R., The Generalized Cattaneo Equation for the Description of Anomalous Transport Processes, *J. Phys. A*, **30(21)**: 72-77 (1997).

[26] Straughan B., Thermal Convection with the Cattaneo-Christov Model, *Int. J. Heat Mass Trans.*, **53**: 95-98 (2010).

[27] Tibullo V., Zampoli V., A Uniqueness Result for the Cattaneo---Christov Heat Conduction Model Applied to Incompressible Fluids, *Mech. Res. Commun.*, **38**: 77-79 (2011).

[28] Haddad S.A.M, Thermal Instability in Brinkman Porous Media with Cattaneo--Christov Heat Flux, *Int. J. Heat Mass Trans.*, **68**: 659-668 (2014).

[29] Reddy J.N., "An Introduction to the Finite Element Method", New York (1993).

[30] Sheikholeslami M, Seyednezhad M., Simulation of Nanofluid Flow and Natural Convection in a Porous Media Under the Influence of Electric Field Using CVFEM, *Int. J. Heat Mass Trans.*, **120**: 772-81 (2018).

[31] Sheikholeslami M., Ghasemi A., Solidification Heat Transfer of Nanofluid in Existence of Thermal Radiation by Means of FEM, *Int. J. Heat Mass Trans*, **123**: 418-31 (2018).

[32] Sheikholeslami M, Finite Element Method for PCM Solidification in Existence of CuO Nanoparticles, *J. Mol. Liq.*, **265**: 347-55 (2018).

[33] Ashraf M.B., Hayat T., Alsaedi A., Three-Dimensional Flow of Eyring-Powell Nanofluid by Convectively Heated Exponentially Stretching Sheet, *Eur. Phys. J. Plus,* **130**: 5 (2015).

[34] Malik M.Y., Khan I., Hussain A., Salahuddin T., Mixed Convection Flow of MHD Eyring-Powell Nanofluid over a Stretching Sheet: A Numerical Study, *AIP Adv.*, **5(11):** 117-118 (2015).

[35] Rubab K, Mustafa M., Cattaneo-Christov Heat Flux Model for MHD Three-Dimensional Flow of Maxwell Fluid over a Stretching Sheet, *PloS One*, **11(4)**: e0153481 (2016).